Schizophrenia Bulletin vol. 50 no. 6 pp. 1396–1410, 2024
https://doi.org/10.1093/schbul/sbae060
Advance Access publication November 1, 2024

Evaluation of the Glymphatic System in Schizophrenia Spectrum Disorder Using Proton Magnetic Resonance Spectroscopy Measurement of Brain Macromolecule and Diffusion Tensor Image Analysis Along the Perivascular Space Index

Ali Abdolizadeh[1,2,], Edgardo Torres-Carmona[1,2], Yasaman Kambari[1,2], Aron Amaev[1,2], Jianmeng Song[1,2], Fumihiko Ueno[1,3,4,], Teruki Koizumi[1,3,5], Shinichiro Nakajima[1,4], Sri Mahavir Agarwal[2,3], Vincenzo De Luca[2,3], Philip Gerretsen[1,2,3,6], and Ariel Graff-Guerrero[1,2,3,6,*]

[1]Multimodal Imaging Group, Research Imaging Centre, Centre for Addiction and Mental Health (CAMH), Toronto, ON, Canada; [2]Institute of Medical Science, Temerty Faculty of Medicine, University of Toronto, Toronto, ON, Canada; [3]Department of Psychiatry, University of Toronto, Toronto, ON, Canada; [4]Department of Neuropsychiatry, Keio University School of Medicine, Tokyo, Japan; [5]Department of Psychiatry, National Hospital Organization Shimofusa Psychiatric Medical Center, Chiba, Japan; [6]Campbell Family Mental Health Research Institute, CAMH, Toronto, ON, Canada

[*]To whom correspondence should be addressed; 80 Workman Way, 6th floor Office 6316, Toronto, ON M6J 1H4, Canada; tel: 416-535-8501, e-mail: Ariel.Graff@camh.ca

***Background and Hypothesis*: The glymphatic system (GS), a brain waste clearance pathway, is disrupted in various neurodegenerative and vascular diseases. As schizophrenia shares clinical characteristics with these conditions, we hypothesized GS disruptions in patients with schizophrenia spectrum disorder (SCZ-SD), reflected in increased brain macromolecule (MM) and decreased diffusion-tensor-image-analysis along the perivascular space (DTI-ALPS) index. *Study Design*: Forty-seven healthy controls (HCs) and 103 patients with SCZ-SD were studied. Data included 135 proton magnetic resonance spectroscopy (^{1}H-MRS) sets, 96 DTI sets, with 79 participants contributing both. MM levels were quantified in the dorsal-anterior cingulate cortex (dACC), dorsolateral prefrontal cortex, and dorsal caudate (point resolved spectroscopy, echo-time = 35ms). Diffusivities in the projection and association fibers near the lateral ventricle were measured to calculate DTI-ALPS indices. General linear models were performed, adjusting for age, sex, and smoking. Correlation analyses examined relationships with age, illness duration, and symptoms severity. *Study Results*: MM levels were not different between patients and HCs. However, left, right, and bilateral DTI-ALPS indices were lower in patients compared with HCs ($P < .001$). In HCs, age was positively correlated with dACC MM and negatively correlated with left, right, and bilateral DTI-ALPS indices ($P < .001$). In patients, illness duration was positively correlated with dACC MM and negatively correlated with the right DTI-ALPS index ($P < .05$). In the entire population, dACC MM and DTI-ALPS indices showed an inverse correlation ($P < .01$). *Conclusions*: Our results suggest potential disruptions in the GS of patients with SCZ-SD. Improving brain's waste clearance may offer a potential therapeutic approach for patients with SCZ-SD.**

Key words: schizophrenia/glymphatic clearance/waste accumulation/macromolecule/DTI-ALPS

Introduction

Despite the high metabolic rate in the brain,[1] the central nervous system lacks the conventional lymphatic system. Instead, the brain possesses a glial-dependent waste drainage pathway called the glymphatic system (GS).[2] In the GS, a combination of cerebrospinal fluid (CSF) pressure gradients, cerebral artery pulsations,[3,4] and respiration[5,6] drives the CSF influx from subarachnoid space into the brain parenchyma along the arterial perivascular space.[7] Diffusion or convective flow mediated by aquaporin-4 (AQP-4) water channels expressed at astrocytic end-feet facilitates the exchange of CSF with interstitial fluid (ISF) in the brain. The ensuing CSF-ISF exchange and metabolite wastes reach the perivenous space, where they are discharged back into the meningeal lymphatic system or deep cervical lymph nodes[8,9] (figure 1).

Dysfunctionality of the GS may reflect anomalies in AQP-4, astroglial dysfunction, arterial stiffness, reduced

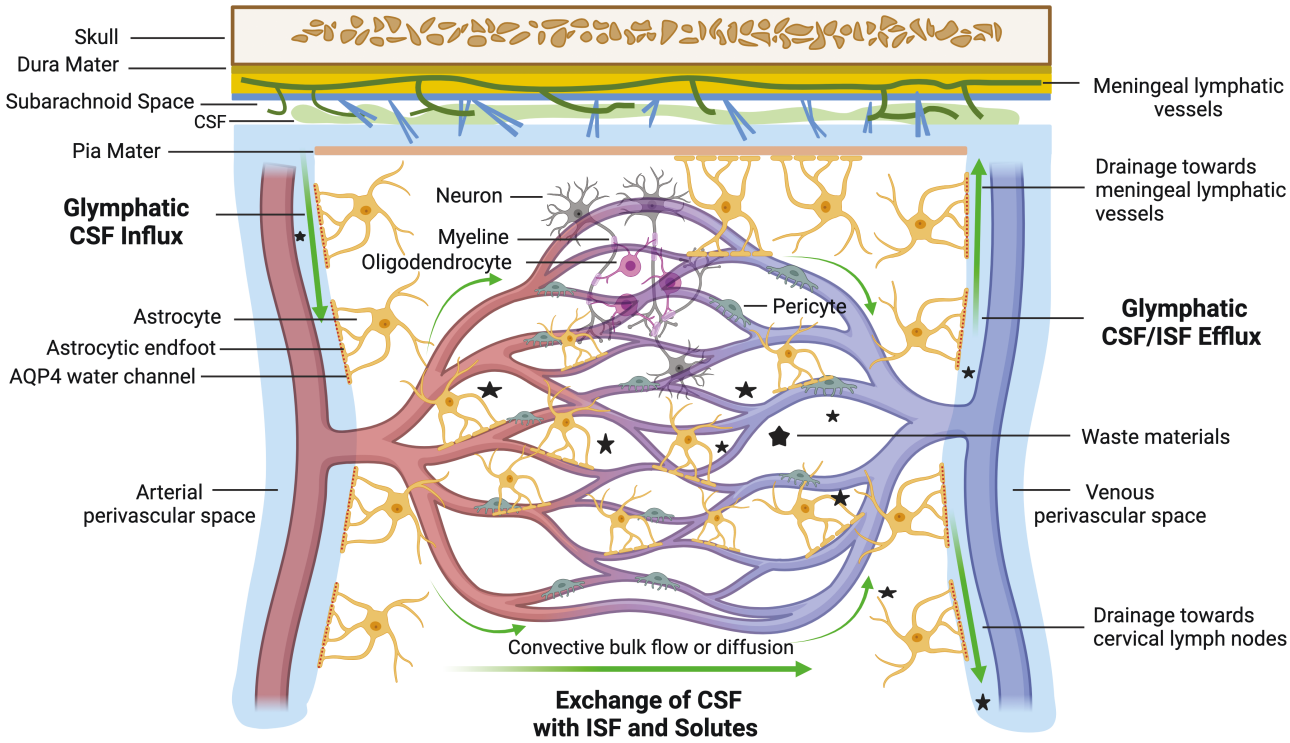

Fig. 1. Schematic representation of the glymphatic system. CSF from the subarachnoid space enters the brain parenchyma along the arterial perivascular space. Either diffusion or convective bulk flow mediated by AQP-4 water channels present at astrocytice end-feet facilitates the exchange of CSF with ISF and solutes. The resulting CSF-ISF fluid exchange and waste materials, through the gaps between astrocytic endfeet, exit along the venous perivascular space towards the meningeal lymphatic system or cervical lymph nodes. Abbreviations: CSF, Cerebrospinal Fluid; AQP, Aquaporine; ISF, Interstitial Fluid. The image was created with BioRender.com.

arterial pulsatility and CSF production, accumulation of brain waste, and lower diffusivity along the perivascular space.[10–17] Various neurodegenerative diseases[18,19] including Alzheimer's disease (AD),[11,20] idiopathic normal pressure hydrocephalus,[10,21] (iNPH), and neurovascular diseases[22,23] exhibit disrupted GS. Additionally, the GS becomes less efficient with aging,[24] and abnormal sleep[25,26] However, the GS has not been explored in schizophrenia spectrum disorders (SCZ-SD).

SCZ is a severe and chronic mental disorder that affects roughly 1% of the population and is characterized by psychotic, negative, and cognitive symptoms.[27,28] It presents features of accelerated biological brain aging,[29–32] cognitive decline, premature death, and metabolic anomalies since prodromal stages.[33–39] Genetic variations of AQP-4 have been correlated with SCZ,[40] and there has been an association between elevated brain pulsations and psychotic-like symptoms.[41] These features are also present in neurodegenerative diseases with impaired GS.[9,42–50] Furthermore, the inverse correlation between choroid plexus (CP) volume and glymphatic clearance rate may reflect neurodevelopmental etiology of disrupted GS.[51] Recent studies also demonstrated increased CP volume associated with proinflammatory markers and psychosis phenomenology across the psychosis spectrum,[52] as well as increased CP variability and lateral ventricle volume in SCZ-SD.[53] This cumulative evidence suggests possible disruptions in the GS of patients with SCZ-SD.

Dynamic contrast-enhanced magnetic resonance imaging (DC-MRI) stands as the most robust approach to study GS.[54,55] However, intrathecal or intravenous administration of gadolinium-based contrast agents into the CSF may lead to neurotoxic effects.[56–59] Thus, in our exploratory study, we aimed to noninvasively evaluate the GS in patients with SCZ-SD and healthy controls (HCs) using proton magnetic resonance spectroscopy (^{1}H-MRS) measurement of brain macromolecule (MM) and diffusion-tensor-image analysis along the perivascular space (DTI-ALPS).

MM peaks in the ^{1}H-spectrum mainly arising from different amino acids are often considered as noises overlapping with neurometabolite signals.[60] However, MM could serve as potential biomarkers for various diseases.[61–63] Further, as implicated in the progression of neurodegenerative diseases, increased oxidative stress-induced cellular damage of MM and insufficient protein repair may contribute to brain aging in SCZ.[16,29,30,64,65] While it is not clear if MM peaks of ^{1}H-spectrum reflect the primary cause of oxidative stress, the aggregation of brain MM, attributed to impaired GS, has been reported in patients with iNPH.[10] We hypothesized increased MM levels in patients with SCZ-SD relative to HCs, which

would be associated with symptom severity and illness duration.

The DTI-ALPS approach, which has been validated with DC-MRI,[22] is a noninvasive technique to assess ISF dynamics by evaluating water diffusivity in the direction of perivascular spaces of medullary veins.[17] A lower DTI-ALPS index observed in AD,[17] Parkinson's disease,[19] iNPH,[21] and cerebral small vessel diseases,[22] reflects reduced glymphatic fluid transport in the brain. We hypothesized decreased DTI-ALPS indices in patients with SCZ-SD relative to HCs, which would be associated with symptom severity and illness duration.

Moreover, we hypothesized that age would be positively associated with MM levels and negatively associated with DTI-ALPS indices in HCs given an age-related decline in the glymphatic function.[24,66] Further, reduced glymphatic fluid transport reflected by lower DTI-ALPS indices could result in the accumulation of brain waste, possibly reflected in increased MM peaks of ^{1}H-spectrum. Thus, we hypothesized an inverse relationship between MM levels and DTI-ALPS indices in the entire population.

Methods

Participants

This exploratory study was carried out at the Center for Addiction and Mental Health (CAMH), Toronto, Ontario, Canada, from 2014 to 2022. The study was approved by the Research Ethics Board at CAMH. The participants provided informed consent. Patients diagnosed with SCZ-SD, as assessed by the structured clinical interview for the Diagnostic and Statistical Manual of Mental Disorders, 4th edition (DSM-IV),[67] were included in the study. HC participants fulfilled the inclusion criteria if they had no history of psychiatric disorders based on the Mini-International Neuropsychiatric Interview (M.I.N.I).[68] HC participants were recruited as closely as possible for age and sex to patient groups. Participants were excluded from the study if they had the following: (a) neurological disorders or severe physical problems, (b) substance dependence or abuse in the past 6 months, (b) history of head trauma associated with loss of consciousness, (c) current treatment with topiramate, memantine, or lamotrigine as our large data set aimed to primarily examine glutamate levels and these meditations are involved in modulating glutamate receptors, or (d) positive urine drug test before scanning. Participants partly overlapped with previously published studies, where more details on the inclusion/exclusion criteria are explained.[69,70]

Magnetic Resonance Imaging

A 3-Tesla GE Discovery MR750 scanner (General Electric, Waukesha, W1) with an 8-channel head coil was used for scanning the participants. Individuals underwent a 3D inversion recovery (IR)-prepared T1-weighted (T1W) magnetic resonance imaging (MRI) (BRAVO; GE Healthcare, Wauwatosa, WI) with the following parameters: repetition time (TR) = 6.74 ms, echo-time (TE) = 3.00 ms, inversion time (TI) = 650 ms, flip angle = 8 °C, field of view = 230 mm, 256 × 256 matrix, slice thickness = 0.9 mm.

Proton Magnetic Resonance Spectroscopy

^{1}H-MRS was acquired with the use of point-resolved spectroscopy (TE = 35 ms, TR = 2000 ms, spectral width = 5000 Hz, 4096 datapoints, 128 water-suppressed, 16 water-unsuppressed averages, and 8 number of excitations). The shimming process was conducted to reach a full width at half maximum ≤ 12 Hz measured on the unsuppressed water signal from the voxel.

^{1}H-MRS voxels were placed in 3 brain areas: bilateral dorsal-anterior cingulate cortex (dACC) (voxel size = 9.0 ml [3.0 × 2.0 × 1.5 cm^3]), left dorsolateral prefrontal cortex (DLPFC) (voxel size = 13.5 ml [3.0 × 3.0 × 1.5 cm^3]), and left-dorsal caudate (associative striatum) (voxel size = 7.5 mL [2.5 × 1.5 × 2.0 cm^3]).[69] It is important to mention that due to the scarcity of the available data, it is not clear whether these specific regions are involved in the glymphatic clearance process or if the ^{1}H-spectrum of MM in these areas can reflect glymphatic function. However, abnormality of dACC, DLPFC, and dorsal caudate has been reported in conditions such as dementia associated with cognitive decline and impaired GS.[71–75] In addition, gray matter atrophy in these areas has been recently shown to be correlated with the DTI-ALPS index in patients with young-onset AD.[76] Given that dACC, DLPFC, and dorsal caudate are also implicated in the pathogenesis of SCZ,[77–85] the ^{1}H-spectrum of MM in these brain areas was investigated in our exploratory study.

FIRST tool[86] in FMRIB Software Library (FSL, version 5.0)[87] was used to segment T1-weighted MRI scans into gray matter, white matter, and cerebrospinal fluid (CSF). A mask of the voxel location and size was applied on the segmented T1-weighted MRI scans using the software package "Gannet" (http://www.gabamrs.com) in MATLAB (The MathWorks, Inc., Natick, MA). LCModel version 6.3-0E was utilized for analyzing the water-suppressed spectra.[88]

Data were analyzed using LCModel for MM quantification and tissue-corrected for CSF fraction. LCModel spectra were visually evaluated, and obvious imaging or spectroscopy artefacts were excluded. Overall, MM at 0.9 ppm (MM09) and 2.0 ppm (MM20) showed lower quantification uncertainties (Cramer-Rao Lower Bound (CRLB) SD ≤ 15%). Therefore, to improve reliability, only participants with at least one brain MM09 and/or MM20 with CRLB SD ≤ 15% were included, and other MM peaks (eg, MM at 1.4 ppm, 1.7 ppm, etc.) were not included in the analysis.

Diffusion Tensor Imaging

Diffusion tensor imaging (DTI) was determined as follows: spin echo-planar imaging, *b*-value = 1000 s/mm^2; 30 directions, 3 volumes were acquired without diffusion weighting (*b*-value = 0 s/mm^2), posterior-to-anterior phase encode direction, TE = 81 ms, TR = 8800 ms, field of view = 100 mm, matrix = 128 × 128, slice thickness = 2 mm.

The raw DTI data were converted from DICOM to NIFTI format using the dcm2nii.exe toolkit included with MRIcroN software (https://www.nitrc.org/projects/mricron). The software automatically created *b*-value and *b*-vector files. FSL (version 6.0) was used for processing steps and DTI-ALPS index calculation.[87] The brain extraction toolbox was utilized to extract the brain from nonbrain regions and create a brain mask for the $b = 0$ images as a template for eddy correction.[89] The diffusion-weighted images were corrected for eddy currents-induced distortions generated from the rapid switching of the diffusing weighting gradients using the *eddy function.*[90] The *repol function* was used, in conjunction with *eddy function*, to detect dropout slices due to the subject movements being coincident with the time of diffusion encoding part of the sequence and replace them with Gaussian process prediction.[91]

Corrected diffusion-weighted data, gradient directions, and values and binary brain masks were imported into DTIFIT (the FSL diffusion tensor fitting program) in the FDT diffusion tool to estimate a diffusion tensor at each voxel. The program generated a series of images including fractional anisotropy (FA) map and diffusivity maps in the direction of the x-axis (left-right; Dx), y-axis (posterior-anterior; Dy), and z-axis (inferior-superior; Dz) for each participant. The FA map was then overlaid with the primary eigenvector (V1) to generate a color-coded FA map for region of interest (ROI) selection.

To reduce the effects of imaging plane and head position, the FA map of all participants was registered to the 1mm-isovoxwl ICBM FA template with 6°C of freedom rigid transformation. Transformation matrices were calculated using *flirt function.*[92–94] The *vecreg function* using registration matrices of FA map was utilized to register the vector data to the ICBM template, creating reoriented diffusivity maps (Dx, Dy, Dz) and colour-coded map (Supplementary figure S1). The reorientation applied to the diffusivity map corrected the *x*-, *y*-, and *z* directions of diffusivity fitted to each brain allowed further validity in the analysis of participants with head rotation.[92,95] The accuracy of coregistration was visually assessed.

ROI Selection and DTI-ALPS Index Calculation

The direction of the perivascular space corresponding to the passing direction of the medullary veins in the deep white matter is perpendicular (*x*-axis) to the ventricle wall at the level of the lateral ventricle body. This direction is also perpendicular to the direction of projection fibers, mainly on the *z*-axis and association fibers, mainly on the *y*-axis. Therefore, the diffusivity along the perivascular space is calculated by the diffusivity along the *x*-axis at regions where both projection and association fibers are present as these major fiber tracts do not run parallel to the direction of the perivascular space (Supplementary figure S2).

The ROI placement was performed only on diffusion-weighted images due to the similarity in the direction of medullary veins, particularly, at the uppermost layer of the lateral ventricle body.[22,96] Thus, we can calculate the DTI-ALPS index on DTI, which has been validated with the glymphatic clearance function measured by glymphatic MRI following intrathecal administration of gadolinium.[22]

Four spherical ROIs with 4-mm-diameter were manually placed in the bilateral projection fibers and association fibers at the uppermost layer of the lateral ventricle body on the color-coded FA map registered to the ICBM FA template (Supplementary figure S3). Diffusivity maps of each participant were overlaid with labels of the periventricular projection fibers (superior/posterior corona radiata) and association fibers (superior longitudinal fasciculus) in ICBM DTI-81 Atlas for further accuracy. Montreal Neurological Institute (MNI) coordinates for the centers of the left ROIs in projection fibers area and association fibers were [−24, −13, 24] and [−36, −13, 24], respectively. MNI coordinates for centers of the right ROIs in the projection fibers area and association fibers area were [24, −13, 24] and [36, −13, 24], respectively. Manual adjustments were applied to confirm the accuracy of the location of ROIs for each participant, and to improve the reproducibility of DTI-ALPS index calculation.

The diffusivities in the directions of the *x*-axis, *y*-axis, and *z*-axis of ROIs on periventricular projection and association areas were recorded as follows: $D_{x\text{proj}}$, $D_{y\text{proj}}$, $D_{z\text{proj}}$, $D_{x\text{assoc}}$, *D*yassoc, and *D*zassoc, respectively. The DTI-ALPS index was calculated as the ratio of the mean of *x*-axis diffusivity in projection fibers and association fibers area (D_{xx}) to the mean of *y*-axis diffusivity in projection fibers area and *z*-axis diffusivity in association fibers area (D_{yz}) as follows: DTI-ALPS Index = $\frac{(Dx\text{proj} + Dx\text{assoc})/2}{(Dy\text{proj} + Dz\text{assoc})/2}$. The averaged value of the left and right DTI-ALPS indices was then calculated.

Statistical Analysis

Statistical analyses were conducted using SPSS statistics version 27 (IBM Corp., Armonk, NY). Independent samples for continuous variables and chi-square test for categorical variables were performed to compare clinical and demographic characteristics between groups. For both ^{1}H-MRS and DTI analyses, the Shapiro–Wilk tests were performed to test the normality of the data and they

confirmed the normal distribution ($P > .05$). Only extreme outliers, defined as values beyond the range of 3rd quartile + 3 * interquartile range and 1st quartile—3 * interquartile range were removed using Tukey's method.[97] Milder outliers that may be the characteristics of the distribution were remained for the analysis, avoiding a false impression of the population.

For primary analyses, independent samples *t*-test was conducted to examine the between-group differences in brain MM levels as well as left, right, and bilateral DTI-ALPS indices. Analysis of covarianece (ANCOVA) was then performed to account for covariates including age, sex, and smoking. This may provide a better estimate and reduce the bias due to confounding. Particularly, controlling the influence of age is assumed to be important for between-group comparisons since it is thought that the GS becomes less efficient in aging. To test our hypothesis regarding the between-group comparisons of MM levels, a significant level of $P < .0166$ (.05/3) was used due to the number of comparisons (each MM in 3 ROIs). To test our hypothesis regarding the between-group comparisons of DTI-ALPS indices, a significant level of $P < .0166$ (.05/3) was used due to the number of comparisons (DTI-ALPS index in 3 ROIs). Partial eta-squared (η_p^2) statistics as a measure of effect size was calculated. Observed power for all the group-wise differences was calculated. If group-wise differences were not sufficiently powered, a priori power test was performed to determine the required sample size for true detection of differences using G*Power software (Version 3.1.9.6, psychologie.hhu.de).[98]

For secondary analyses, bivariate and/or partial correlation analyses were investigated. Bivariate correlation analysis assesses the relationship between 2 variables without considering the influence of other variables. In contrast, partial correlation analysis allows us to assess the relationship between variables while controlling for potential confounding factors. We used bivariate correlation analysis to examine the associations between age and both MM levels and DTI-ALPS indices in HC participants using a significant threshold of $P < .0166$ (.05/3) due to the number of comparisons (each MM in 3 ROIs or DTI-ALPS index in 3 ROIs * age), as an external validity for our analyses. Bivariate correlations between MM levels and DTI-ALPS indices were also explored in the entire population to test a construct validity for our methods using a significant threshold of $P < .0055$ (.05/9) due to the number of comparisons (each MM in 3 ROIs * DTI-ALPS index in 3 ROIs). In the whole patient sample, bivariate correlation, and partial correlation analyses, adjusted for age, sex, and smoking were performed to examine the relationship between illness duration and both MM levels and DTI-ALPS indices using a significant threshold of $P < .0166$ (.05/3) due to the number of comparisons (each MM in 3 ROIs or DTI-ALPS index in 3 ROIs * illness duration). The relationship between symptoms severity as measured by Positive and Negative Syndrome Scale (PANSS)[99] and both MM levels and DTI-ALPS indices were also explored using a significant threshold of $P < .0042$ (.05/12) due to the number of comparisons (each MM in 3 ROIs or DTI-ALPS index in 3 ROIs * 4 PANSS total, positive, negative, and general subscales).

Results

The entire sample in our exploratory study consisted of 150 participants, 103 patients with SCZ-SD and 47 HC participants. The mean age for the entire sample was 43.72 (±13.53), which was largely composed of male subjects ($n = 115$, 76.7%) (Table 1). Of these, 135 participants had ^{1}H-MRS data contributing to the MM analyses and 96 participants had DTI data contributing to the DTI-ALPS analyses. Among them, 79 had both ^{1}H-MRS and DTI data allowing for within-subject comparisons between MM and DTI-ALPS indices. The detailed clinicodemographic characteristics of participants included in each analysis are shown in Supplementary table S1 and S2.

^{1}H-MRS Study

Group-Wise Comparison of Brain MM. Table 2 shows the level of MM09 and MM20 in the bilateral dACC, left DLPFC, and left dorsal caudate with summary statistics. While there was a trend toward increased brain MM in patients with SCZ-SD relative to HCs, the level of MM09 and MM20 did not significantly differ between groups, even when we controlled for covariates including age, sex, and smoking status. However, between-group differences in brain MMs were not sufficiently powered. To detect a medium effect size (Cohen's $d = 0.5$) with 80% power in an independent samples *t*-test (2 groups, alpha = 0.05), G*Power suggests we would need a total of 128 participants (64 per group).

Correlations With Brain MM. Age was positively associated with the MM20 in the bilateral dACC in HCs ($r = 0.552$, $P < .001$, $n = 44$) (figure 2). Relationships between age and other MMs were not statistically significant. Additionally, age was not associated with brain MMs in patients with SCZ-SD.

Illness duration was positively associated with the MM09 ($r = 0.328$, $P = .002$, $n = 86$) and MM20 ($r = 0.374$, $P < .001$, $n = 85$) in the bilateral dACC of the entire patient group. The results of partial correlation analyses, adjusted for age, sex, and smoking status, also showed a positive correlation between illness duration and the MM09 ($r = 0.356$, $P < .001$, $n = 86$) and MM20 ($r = 0.280$, $P = .011$, $n = 85$) in the bilateral dACC (figure 2). Relationships between illness duration and other MMs were not statistically significant. There was no correlation between brain MM levels and symptom severity.

Table 1. Demographics of the entire population included in MM and/or DTI analyses. Values are reported as mean (±SD) or *n* (%). [a]HC group had higher years of education than SCZ-SD group; [b]HC group had higher ratio of nonsmokers to smokers than SCZ-SD group ($P < .001$).

			t-Test or Chi Square	
	SCZ-SD ($n = 103$)	HC ($n = 47$)	*t* Value or df	*P* value
Age, y	44.16 (± 12.868)	42.77 (± 14.97)	$t(148) = 0.582$	.281
Sex, female/male	23 (22.3)/80 (77.7)	12 (25.5)/35 (74.5)	1	.667
Education, y	12.94 (± 2.87)	16.38 (± 2.46)	$t(148) = 7.110$	<.001[a]
Cigarette, users/nonusers	54 (52.4)/ 49 (47.6)	1 (2.1)/ 46 (97.90)	1	<.001[b]
Age of onset, y	23.39 (± 6.373)	N/A	N/A	N/A
Illness duration, y	20.60 (± 12.283)	N/A	N/A	N/A
PANSS total score	64.66 (± 16.99)	N/A	N/A	N/A
Positive subscale	15.12 (± 6.25)	N/A	N/A	N/A
Negative subscale	17.45 (± 4.9)	N/A	N/A	N/A
General subscale	32.13 (± 7.90)	N/A	N/A	N/A

Note: HC, healthy control; PANSS, Positive and Negative Syndrome Scale; SCZ-SD, Schizophrenia Spectrum Disorder; SD, standard deviation.

DTI Study

Group-Wise Comparison of DTI-ALPS Indices. The DTI-ALPS index in the left hemisphere ($P < .001$), right hemisphere ($P < .001$), and averaged DTI-ALPS index from the left and right hemispheres ($P < .001$) were lower in the patient group compared to HCs. The results remained statistically significant after including age, sex, and smoking status as covariates ($P < .001$) (table 3). Supplementary table S3 shows the diffusivity values used to calculate DTI-ALPS indices.

Correlations With DTI-ALPS Indices. Age was inversely associated with the left DTI-ALPS index ($r = -0.705$, $P < .001$, $n = 25$), right DTI-ALPS index ($r = -0.427$, $P < .001$, $n = 25$), and averaged DTI-ALPS index from the left and right hemispheres ($r = -0.652$, $P < .001$, $n = 25$) in HCs. However, there was no correlation between age and DTI-ALPS indices in patients with SCZ-SD (figure 2).

While bivariate correlation did not find associations between illness duration and DTI-ALPS indices, partial correlation analyses, corrected for age, sex, and smoking status revealed that illness duration was inversely associated with only the right DTI-ALPS index ($r = -0.313$, $P = .009$, $n = 71$) (figure 2). There was no association between DTI-ALPS indices and symptom severity.

Relationships Between Brain MM and DTI-ALPS Indices

In the entire population, the MM09 in the dACC was inversely correlated with the left DTI-ALPS index ($r = -0.342$, $P = .002$, $n = 79$), right DTI-ALPS index ($r = -0.499$, $P < .001$, $n = 79$), and averaged DTI-ALPS index from the left and right hemispheres ($r = -0.469$, $P < .001$, $n = 79$) (figure 2). While not statistically significant considering Bonferroni-correction for multiple comparisons, similar pattern was observed for the MM20 in the dACC showing an inverse relationship with the left DTI-ALPS index ($r = -0.220$, $P = .05$, $n = 79$), right DTI-ALPS index ($r = -0.279$, $P = .013$, $n = 79$), and averaged DTI-ALPS index from the left and right hemispheres ($r = -0.278$, $P = .013$, $n = 79$). There was no association between MM in the DLPFC or left caudate and DTI-ALPS indices.

Discussion

To the best of our knowledge, our exploratory study is the first to explore the GS in patients with SCZ-SD. The results support the external validity of our approach, revealing relationships between age and both MM and DTI-ALPS indices in HCs. Additionally, the inverse relationship between MM and DTI-ALPS indices in our within-subject study provides a valid construct for our methods. Our results provide evidence for our hypothesis, as we observed decreased DTI-ALPS indices in patients with SCZ-SD compared to HCs. We also identified a negative correlation between the right DTI-ALPS index and illness duration, along with a positive correlation between MM and illness duration. However, it is important to note that no significant differences in brain MM were found between patients and HCs.

Relationship Between Age and Both MM and DTI-ALPS Indices

Age was positively correlated with MMs in the dACC and negatively correlated with DTI-ALPS indices in HCs, providing external validation for our analyses. This aligns with previous studies, indicating that the efficiency of the GS declines with age,[24,66] attributed to astroglial dysfunction and AQP-4 channels depolarization,[24] arterial stiffness, reduced arterial pulsatility, and CSF production.[15,16] There was no correlations between age and MM or DTI-ALPS indices in patients, which could be explained by possible disruptions in the GS of patients with SCZ-SD.

Table 2. Comparison of macromolecule levels between patients with SCZ-SD and HC participants. Only MMs with Cramer-Rao Lower Bound (CRLB) SD ≤ 15% were included in the analysis. [a]Age, sex, and smoking status were included as covariates. Values are reported as mean (SE). Partial eta-squared values of approximately 0.01, 0.06, and 0.14 signify small, medium, and large effect sizes, respectively.

				t-test					ANCOVA[a]				
		SCZ-SD	HC	*t* Value	*P* value	Partial eta-squared	Noncent. Parameter	Observed Power	F value	*P* value	Partial eta-squared	Noncent. Parameter	Observed Power
MM09	**dACC**	*n* = 87 9.30 (0.21) 95% CI [8.89–9.71]	*n* = 44 8.92 (0.29) 95% CI [8.34–9.51]	*t*(129) = −1.050	.296	0.008	1.102	0.181	$F_{1,126}$ = 1.014	.419	0.008	1.014	0.170
	DLPFC	*n* = 80 8.25 (0.39) 95% CI [7.47–0.03]	*n* = 42 7.58 (0.54) 95% CI [6.51–8.65]	*t*(120) = −1.003	.318	0.008	1.006	0.169	$F_{1,117}$ = 1.137	.288	0.010	1.137	0.185
	DC	*n* = 75 6.32 (0.19) 95% CI [5.94–6.71]	*n* = 40 6.50 (0.26) 95% CI [5.97–7.02]	*t*(113) = 0.536	.593	0.003	0.287	0.083	$F_{1,110}$ = 0.480	.490	0.004	0.480	0.105
MM20	**dACC**	*n* = 86 18.61 (0.33) 95% CI [17.95-19.28]	*n* = 44 17.61 (0.47) 95% CI [16.68-18.53]	*t*(128) = −1.747	.083	0.023	3.051	0.411	$F_{1,125}$ = 2.434	.121	0.019	2.434	0.340
	DLPFC	*n* = 79 13.86 (0.23) 95% CI [13.40–14.32]	*n* = 42 13.35 (0.32) 95% CI [12.71–13.98]	*t*(119) = −1.299	.197	0.014	1.686	0.251	$F_{1,116}$ = 0.955	.330	0.008	0.995	0.163
	DC	*n* = 52 12.92 (0.31) 95% CI [12.30–13.54]	*n* = 31 12.64 (0.40) 95% CI [11.84–13.45]	*t*(81) = −0.549	.585	0.004	0.301	0.084	$F_{1,78}$ = 0.618	.434	0.008	0.618	0.121

Note: ANCOVA, analysis of covariance; CI, confidence interval; dACC, dorsal anterior cingulate cortex; DLPFC, dorso-lateral prefrontal cortex; DC: dorsal caudate; MM, macromolecule; SE, standard error.

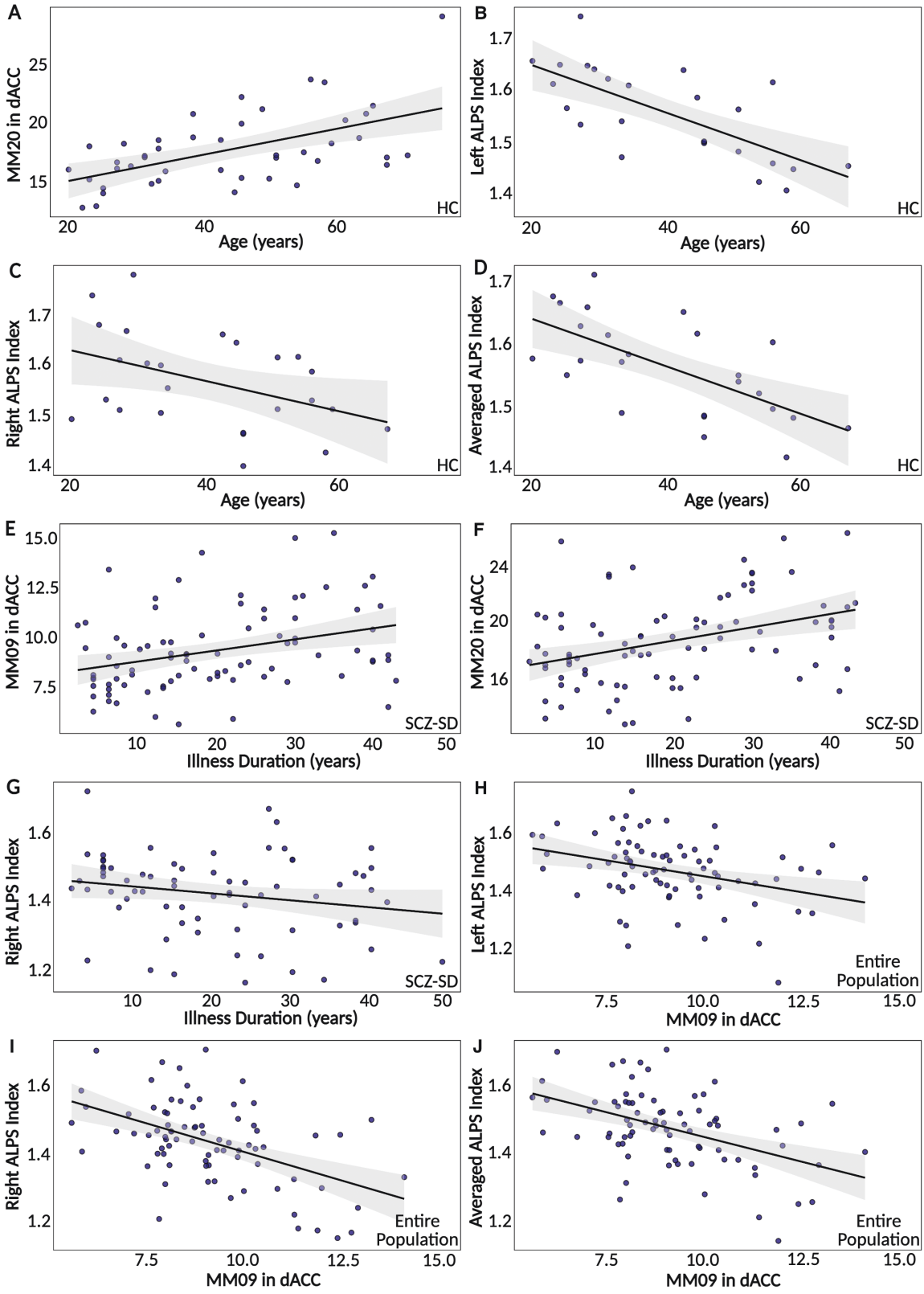

Fig. 2. Correlations of MM levels and DTI-ALPS indices with age and illness duration, and correlations between MM and DTI-ALPS indices. (A) Positive correlation between age and MM20 in the dACC in HC participants ($r = 0.552$, $P < .001$, $n = 44$). (B) Inverse correlation between age and the left DTI-ALPS index in HC participants ($r = -0.705$, $P < .001$, $n = 25$). (C) Inverse correlation between age and the right DTI-ALPS index in HC participants ($r = -0.427$, $P < .001$, $n = 25$). (D) Inverse correlation between age and average of left and right DTI-ALPS indices in HC participants ($r = -0.652$, $P < .001$, $n = 25$). (E) Positive correlation between illness duration and

Relationship Between MM and DTI-ALPS Indices

MM level in the dACC was negatively associated with left, right, and bilateral DTI-ALPS indices in the entire population. This finding suggests that a decreased DTI-ALPS index reflecting impairment in the interstitial fluid dynamics could result in deposition of brain MM, further validating our methods to explore the GS. The absence of correlation between DTI-ALPS indices and MM levels in the DLPFC and dorsal caudate may be attributed to regional variations in glymphatic function. Additionally, factors including differential gray matter atrophy, vascularization, or metabolic activity in these regions could contribute to the observed discrepancies in correlations. Further investigation into the association between gray matter regions and DTI-ALPS indices may provide insights into these variations.

H^1-MRS Measurement of Brain MM

In our exploratory study, despite the numerical increase in the brain MM levels of patients with SCZ-SD compared to HCs, the numerical increase was not statistically different. Although MM peaks observed at ^{1}H-spectrum are not reflective of a particular substance, they mainly arise from protons of overlapping amino acids which are nonspecific to a particular cytosolic protein/peptide.[60]

The reliability of MM quantification may vary according to spectral ranges. While mobile lipids may contribute to the ^{1}H-spectrum due to disease or outer-volume-contamination, the MM09 mainly reflects branched-chain amino acids (leucine, isoleucine, and valine).[60] While the impact of each amino acid in the pathophysiology of SCZ-SD is not clear,[100] peripheral concentration of leucine, isoleucine, and valine may affect precursors for the synthesis of biogenic amines,[101] contributing to imbalances in neurotransmitters norepinephrine, dopamine, serotonin, and histidine, which have been postulated in the pathogenesis of SCZ.[102] Notably, MMs resonating at 2.0–4.0 ppm highly overlap with neurometabolites. The MM20 in the ^{1}H-spectrum might implicate glutamate and glutamine although the specificity of such signal is low.[60] Elevated glutamate–glutamine level in dACC has been reported in patients with SCZ,[69] consistent with the glutamate hypothesis of SCZ.[103,104] However, a meta-analysis demonstrated decreased glutamate but increased glutamine in medial frontal regions of patients with SCZ,[105] implying that the contribution of each amino acid to the ^{1}H-spectrum may vary.[106]

Recently, increased MM at 1.4 and 1.7 ppm was reported in patients with iNPH reflecting impaired GS.[10] However, similar to our findings, MM09 or MM20 was not elevated in patients. Exclusion of MM peaks at 1.4 and 1.7 ppm in our study due to high quantification uncertainties might contribute to the lack of MM accumulation in patients with SCZ-SD. However, in contrast to our study, Akiyama et al explored MM in centrum semiovali. Alterations in MRI measurements of the GS in centrum semiovali has been previously demonstrated,[107–109] suggesting that the location of ^{1}H-MRS voxels for MM quantification may provide different insight. Further, the correlation between illness duration and MM09 and MM20 in dACC may imply that the disease progression alters the MM profile in the ^{1}H-spectrum. The heterogenous nature of SCZ-SD and the variability in treatment response may link the lack of association between symptom severity and MM.

Nevertheless, the evidence from our study is not sufficient to conclude that SCZ-SD is associated with MM accumulation. Future studies exploring MM at different peaks and brain areas including centrum semiovali may elucidate MM aggregation in this patient population. It is also important to acknowledge that MM level is a proxy measure of glymphatic flow and cross-validation between ^{1}H-MRS measurement of MM and other MRI assessments of the GS warrants further investigation.

^{1}H-MRS Limitation

Our ^{1}H-MRS analysis has some limitations: (1) In our cross-sectional study, covariates interactions including medications and sleep could have modulated MM levels; (2) The ^{1}H-MRS sequence lacks specificity for MM and there is poor knowledge regarding specific molecules in each MM resonance. It is also not clear how proportion of MM is considered brain waste. Future study should validate MM findings of ^{1}H-MRS with glymphatic MRI; (3) We only evaluated MM in dACC, DLPFC, and dorsal caudate, potentially missing the impact of MM accumulation in other regions on overall clearance; (4) Only MM peaks at 0.9 ppm and 2.00 ppm were included in the analysis. However, exploring MM levels at other peaks may

MM09 in the dACC in patients with SCZ-SD (r = 0.328, P = .002, n = 86; covariates-corrected, r = 0.356, P < .001, n = 86). (F) Positive correlation between illness duration and MM20 in the dACC in patients with SCZ-SD (r = 0.374, P < .001, n = 85; covariates-corrected, r = 0.280, P = .011, n = 85). (G) Inverse correlation between illness duration and the right DTI-ALPS index in patients with SCZ-SD (r = −0.313, P = .009, n = 71, covariates-corrected). (H) Inverse correlation between MM09 in the dACC and the left DTI-ALPS index in the entire population (r = -0.342, P = .002, n = 79). (I) Inverse correlation between MM09 in the dACC and the right DTI-ALPS index in the entire population (r = −0.499, P < .001, n = 79). (J) Inverse correlation between MM09 in the dACC and the average of left and right DTI-ALPS indices in the entire population (r = −0.496, P < .001, n = 79). Abbreviations: dACC, dorsal anterior cingulate cortex; DTI-ALPS, diffusion tensor image analysis along the perivascular space; HC, healthy control; MM, macromolecule; SCZ-SD, schizophrenia spectrum disorder.

Table 3. Comparison of DTI-ALPS indices between patients with SCZ-SD and HC participants. DTI-ALPS index was calculated as a ratio of mean of *x*-axis diffusivity in projection fibers area and association fibers area (D_{xx}) to mean of *y*-axis diffusivity in projection fibers area and *z*-axis diffusivity in association fibers area (D_{yz}). DTI-ALPS indices for left and right hemispheres were averaged to calculate the bilateral DTI-ALPS index. [a]Age, sex, and smoking status were included as covariates. Values are reported as mean (SE). Partial eta-squared values of approximately 0.01, 0.06, and 0.14 signify small, medium, and large effect sizes, respectively.

			t-test				ANCOVA[a]				
	SCZ-SD (n = 71)	HC (n = 25)	t Value	P Value	Partial eta-squared	Noncent. Parameter	Observed Power	F value	P value	Partial eta-squared	Noncent. Parameter	Observed Power
Left ALPS index	1.45 (0.013) 95% CI [1.422, 1.472]	1.56 (0.021) 95% CI [1.514, 1.599]	$t(94) = 4.436$	< .001	.173	19.674	.992	$F_{1,91} = 12.408$	< .001	.120	12.408	.936
Right ALPS index	1.44 (0.014) 95% CI [1.415, 1.472]	1.57 (0.024) 95% CI [1.519, 1.615]	$t(94) = 4.399$	< .001	.171	19.354	.992	$F_{1,91} = 12.853$	< .001	.124	12.853	.944
Averaged ALPS indices	1.45 (0.012) 95% CI [1.422, 1.469]	1.56 (0.020) 95% CI [1.523, 1.601]	$t(94) = 5.063$	< .001	.214	25.631	.999	$F_{1,91} = 16.715$	< .001	.155	16.715	.981

Note: ALPS, along the perivascular space.

provide different insight; (5) Many group-wise MM differences lacked sufficient power. G* power suggested the total sample size required to detect an effect with 80% power is 128 for between-group comparisons.

DTI-ALPS Indices

In our exploratory study, the reduced DTI-ALPS indices were evident in patients with SCZ-SD, compared to HCs, suggesting possible GS disruptions underlying the pathogenesis of SCZ-SD. Potential contributing factors include enlarged perivascular space,[110] reduced arterial pulsation,[41] altered AQP-4 channels distribution/expression,[40] and astrocytic dysfunction.[111] Moreover, longer illness duration was correlated with a lower DTI-ALPS index. This correlation was observed exclusively in the right hemisphere and only after controlling for covariates. The observed correlation between diseases progression and the DTI-ALPS index prompts further inquiry into the potential implications for illness pathology. By reframing our findings within the context of an exploratory study, we acknowledge the need for additional research to elucidate the complex interplay between the glymphatic system and schizophrenia progression.

Importantly, norepinephrine dysregulation has been postulated in the pathophysiology of SCZ.[112] Norepinephrine in the locus coeruleus-noradrenergic pathway plays important roles in regulating arousal.[7,113] Additionally, norepinephrine may reduce the extracellular space volume and increase the resistance to the CSF influx to the brain parenchyma and CSF-ISF exchange, suppressing the glymphatic fluid transport during wakefulness.[7,25,113] This highlights the contribution of norepinephrine to regulate the sleep-wakefulness switch while influencing the GS. Thus, norepinephrine dysregulation in patients with SCZ-SD my partly explain the reduced DTI-ALPS indices reflecting diminished glymphatic fluid transport in this patient population.

Moreover, dopaminergic neurons in the mesolimbic pathway could modulate arousal during sleep and wakefulness.[114,115] Dysregulation of dopaminergic system, as implicated in the pathogenesis of SCZ,[116–118] may lead to sleep difficulties which indirectly influence the GS. Accordingly, sleep disturbances, partly attributed to dopaminergic system hyperactivity and impaired GABAergic function, are commonly observed in patients with SCZ, which may not significantly improve with antipsychotics.[119] The GS is most active during sleep and sleep disruptions may impede this process,[24,26] and are associated with reduced DTI-ALPS indices.[120] Hence, sleep issues may also contribute to reduced DTI-ALPS indices in patients with SCZ-SD.

The discrepancy in our 2 assessment methods of the GS might be due to the intricate nature of glymphatic dynamics. The ^{1}H-MRS measurement of brain MM at specific peaks in specific brain areas might not capture

the overall complexity of glymphatic function. However, the DTI-ALPS index, which has been correlated with glymphatic DC-MRI, offers a more comprehensive perspective of glymphatic function by assessing fluid transport along perivascular spaces. These findings underscore the need for a multifaceted approach when investigating the GS in SCZ-SD.

DTI-ALPS Limitation

Our DTI analysis has some limitations: (1) medications and their potential effects on sleep might have influenced the DTI-ALPS indices; (2) despite the correlation between DTI-ALPS indices and the glymphatic function measured by glymphatic DC-MRI,[22] careful interpretation is required to determine its relevance to the overall glymphatic function. The glymphatic DC-MRI represents the CSF influx along the arterial perivascular space, CSF-ISF fluid exchange, and CSF-ISF efflux along the venous perivascular space,[22] while the DTI-ALPS index may only represent CSF-ISF efflux; (3) susceptibility weighted images were not used to visualize the fine medullary veins. However, Taoka et al reported high test–retest reproducibility of the DTI-ALPS index without SWI for ROI; (4) despite using atlases and manual adjustments for ROI placement, some subjectivity may still exist; (5) we did not correct for distortions caused by magnetic field inhomogeneities as single encoding direction was applied for DTI acquisition (unable to perform FSL *topup function*) and field mappings were not available (unable to perform FSL *fudge function*).

Conclusion

In summary, the findings of our exploratory study suggest potential GS disruptions underlying the pathogenesis of SCZ-SD. Improving brain's waste clearance may offer a potential therapeutic approach for this patient population. Further well-designed studies using noninvasive methods are required to replicate our findings and to explore other components of the GS in patients with SCZ-SD.

Supplementary Material

Supplementary material is available at https://academic.oup.com/schizophreniabulletin/.

Conflict of interest

The authors have declared that there are no conflicts of interest in relation to the subject of this study.

Funding

Ali Abdolizadeh has nothing to disclose. Edgardo Torres-Carmona has nothing to disclose. Yasaman Kambari has nothing to disclose. Aron Amaev has nothing to disclose. Jianmeng Song has nothing to disclose. Fumihiko Ueno has received research grants from the Brain & Behavior Research Foundation (BBRF); fellowship grants from Discovery Fund, Nakatani Foundation, and the Canadian Institutes of Health Research (CIHR); manuscript fees from Dainippon Sumitomo Pharma; and consultant fees from WCG Clinical, and Uchiyama Underwriting within the past 3 years. Teruki Koizumi has received research grants from the Japanese Society of Clinical Neuropsychopharmacology and the Canadian Institutes of Health Research (CIHR), manuscript fees from Dainippon Sumitomo Pharma; and consultant fees from VeraSci and Signanthealth within the past 3 years. Shinichiro Nakajima has received grants from Japan Society for the Promotion of Science (18H02755, 22H03002), Japan Agency for Medical Research and development (AMED), Japan Research Foundation for Clinical Pharmacology, Naito Foundation, Takeda Science Foundation, Uehara Memorial Foundation, Watanabe Foundation, and Osake-no-Kagaku Foundation; an investigator-initiated clinical study grant from Asahi Quality & Innovations, Ltd; research support, manuscript fees or speaker's honoraria from Sumitomo Pharma, Meiji- Seika Pharma, Otsuka Pharmaceutical, and MSD within the past 3 years. Sri Mahavir Agarwal is supported in part by the CAMH Discovery Fund and an Academic Scholars Award from the Department of Psychiatry, University of Toronto, and has grant support from the CIHR, PSI Foundation, Department of Psychiatry, University of Toronto, Banting & Best Diabetes Centre, University of Toronto, and the CAMH Discovery Fund. He has served as a consultant for HLS therapeutics and Boehringer Ingelheim Canada. Vincenzo De Luca has been supported by a Miner's Lamp Award from the Department of Psychiatry at the University of Toronto, a Scholar Award from the Department of Psychiatry at the University of Toronto the University of Toronto, and a standard research grant from the American Foundation for Suicide Prevention (AFSP) within the last 3 years. Philip Gerretsen has received research support from the Canadian Institute of Health Research (CIHR), Ontario Ministry of Health and Long-Term Care, Ontario Ministry of Colleges and Universities, Ontario Mental Health Foundation (OMHF), the Centre for Addiction and Mental Health (CAMH), CAMH Foundation. He is the inventor of and receives revenue from the commercialization of the VAGUS Scales, Illness Awareness Scales, and Addiction Awareness Scales. Ariel Graff-Guerrero is currently supported by Canadian Institutes of Health Research (CIHR), Banting & Best Diabetes Centre, University of Toronto, CAMH Foundation, Temerty-Tanz-TDRA Seed Fund for Research on Depression and Dementia at the University of Toronto, Ontario AHSC AFP Innovation Fund (MOHLTC).

Data Availability

Data analyzed in this study are available from the corresponding author upon reasonable request.

References

1. Clarke DD, Sokoloff L. Regulation of Cerebral Metabolic Rate. In: *Basic Neurochemistry: Molecular, Cellular and Medical Aspects*. 6th ed. Philadelphia: Lippincott-Raven; 1999. Accessed November 2, 2023. https://www.ncbi.nlm.nih.gov/books/NBK28194/
2. Iliff JJ, Lee H, Yu M, et al. Brain-wide pathway for waste clearance captured by contrast-enhanced MRI. *J Clin Invest.* 2013;123(3):1299–1309. doi:10.1172/JCI67677
3. Iliff JJ, Wang M, Zeppenfeld DM, et al. Cerebral arterial pulsation drives paravascular CSF-interstitial fluid exchange in the murine brain. *J Neurosci.* 2013;33(46):18190–18199. doi:10.1523/JNEUROSCI.1592-13.2013
4. Bilston LE, Stoodley MA, Fletcher DF. The influence of the relative timing of arterial and subarachnoid space pulse waves on spinal perivascular cerebrospinal fluid flow as a possible factor in syrinx development. *J Neurosurg.* 2010;112(4):808–813. doi:10.3171/2009.5.JNS08945
5. Yamada S, Miyazaki M, Yamashita Y, et al. Influence of respiration on cerebrospinal fluid movement using magnetic resonance spin labeling. *Fluids Barriers CNS*. 2013;10(1):36. doi:10.1186/2045-8118-10-36
6. Klose U, Strik C, Kiefer C, Grodd W. Detection of a relation between respiration and CSF pulsation with an echoplanar technique. *J Magn Reson Imaging.* 2000;11(4):438–444. doi:10.1002/(sici)1522-2586(200004)11:4<438::aid-jmri12>3.0.co;2-o
7. Jessen NA, Munk ASF, Lundgaard I, Nedergaard M. The glymphatic system: a beginner's guide. *Neurochem Res.* 2015;40(12):2583–2599. doi:10.1007/s11064-015-1581-6
8. Kaur J, Davoodi-Bojd E, Fahmy LM, et al. Magnetic resonance imaging and modeling of the glymphatic system. *Diagnostics (Basel)*. 2020;10(6):344. doi:10.3390/diagnostics10060344
9. Natale G, Limanaqi F, Busceti CL, et al. Glymphatic system as a gateway to connect neurodegeneration from periphery to CNS. *Front Neurosci.* 2021;15:639140. doi:10.3389/fnins.2021.639140
10. Akiyama Y, Yokoyama R, Takashima H, et al. Accumulation of macromolecules in idiopathic normal pressure hydrocephalus. *Neurol Med Chir (Tokyo)*. 2021;61(3):211–218. doi:10.2176/nmc.oa.2020-0274
11. Iliff JJ, Wang M, Liao Y, et al. A paravascular pathway facilitates CSF flow through the brain parenchyma and the clearance of interstitial solutes, including amyloid β. *Sci Transl Med.* 2012;4(147):147ra111. doi:10.1126/scitranslmed.3003748
12. Zeppenfeld DM, Simon M, Haswell JD, et al. Association of perivascular localization of aquaporin-4 with cognition and Alzheimer disease in aging brains. *JAMA Neurol*. 2017;74(1):91–99. doi:10.1001/jamaneurol.2016.4370
13. Xu Z, Xiao N, Chen Y, et al. Deletion of aquaporin-4 in APP/PS1 mice exacerbates brain Aβ accumulation and memory deficits. *Mol Neurodegener.* 2015;10:58. doi:10.1186/s13024-015-0056-1
14. Gavrilov GV, Stanishevskiy AV, Gaydar BV, Paramonova NM, Gaykova ON, Svistov DV. [Pathological changes in human brain biopsies from patients with idiopathic normal pressure hydrocephalus]. *Zh Nevrol Psikhiatr Im S S Korsakova.* 2019;119(3):50–54. doi:10.17116/jnevro201911903150
15. Zieman SJ, Melenovsky V, Kass DA. Mechanisms, pathophysiology, and therapy of arterial stiffness. *Arterioscler Thromb Vasc Biol.* 2005;25(5):932–943. doi:10.1161/01.ATV.0000160548.78317.29
16. Chen RL, Kassem NA, Redzic ZB, Chen CPC, Segal MB, Preston JE. Age-related changes in choroid plexus and blood–cerebrospinal fluid barrier function in the sheep. *Exp Gerontol.* 2009;44(4):289–296. doi:10.1016/j.exger.2008.12.004
17. Taoka T, Masutani Y, Kawai H, et al. Evaluation of glymphatic system activity with the diffusion MR technique: diffusion tensor image analysis along the perivascular space (DTI-ALPS) in Alzheimer's disease cases. *Jpn J Radiol*. 2017;35(4):172–178. doi:10.1007/s11604-017-0617-z
18. Rasmussen MK, Mestre H, Nedergaard M. The glymphatic pathway in neurological disorders. *Lancet Neurol*. 2018;17(11):1016–1024. doi:10.1016/S1474-4422(18)30318-1
19. Ma X, Li S, Li C, et al. Diffusion tensor imaging along the perivascular space index in different stages of Parkinson's disease. *Front Aging Neurosci.* 2021;13:773951. doi:10.3389/fnagi.2021.773951
20. Peng W, Achariyar TM, Li B, et al. Suppression of glymphatic fluid transport in a mouse model of Alzheimer's disease. *Neurobiol Dis.* 2016;93:215–225. doi:10.1016/j.nbd.2016.05.015
21. Yokota H, Vijayasarathi A, Cekic M, et al. Diagnostic performance of glymphatic system evaluation using diffusion tensor imaging in idiopathic normal pressure hydrocephalus and mimickers. *Curr Gerontol Geriatrics Res*. 2019;2019:1–10. doi:10.1155/2019/5675014
22. Zhang W, Zhou Y, Wang J, et al. Glymphatic clearance function in patients with cerebral small vessel disease. *Neuroimage.* 2021;238:118257. doi:10.1016/j.neuroimage.2021.118257
23. Ji C, Yu X, Xu W, Lenahan C, Tu S, Shao A. The role of glymphatic system in the cerebral edema formation after ischemic stroke. *Exp Neurol.* 2021;340:113685. doi:10.1016/j.expneurol.2021.113685
24. Kress BT, Iliff JJ, Xia M, et al. Impairment of paravascular clearance pathways in the aging brain. *Ann Neurol.* 2014;76(6):845–861. doi:10.1002/ana.24271
25. Xie L, Kang H, Xu Q, et al. Sleep drives metabolite clearance from the adult brain. *Science.* 2013;342(6156):373–377. doi:0.1126/science.1241224. doi:10.1126/science.1241224
26. Nedergaard M, Goldman SA. Brain drain. *Sci Am.* 2016;314(3):44–49. doi:10.1038/scientificamerican0316-44
27. Jauhar S, Johnstone M, McKenna PJS. Schizophrenia. *The Lancet*. 2022;399(10323):473–486. doi:10.1016/S0140-6736(21)01730-X
28. McGrath J, Saha S, Chant D, Welham JS. A concise overview of incidence, prevalence, and mortality. *Epidemiol Rev.* 2008;30(1):67–76. doi:10.1093/epirev/mxn001
29. Kirkpatrick B, Messias E, Harvey PD, Fernandez-Egea E, Bowie CR. Is schizophrenia a syndrome of accelerated aging? *Schizophr Bull.* 2008;34(6):1024–1032. doi:10.1093/schbul/sbm140
30. Okusaga O. Accelerated aging in schizophrenia patients: the potential role of oxidative stress. *Aging Dis*. 2014;256:256–262. doi:10.14336/AD.2014.0500256
31. Seeman MV. Subjective overview of accelerated aging in schizophrenia. *IJERPH*. 2022;20(1):737. doi:10.3390/ijerph20010737
32. Campeau A, Mills RH, Stevens T, et al. Multi-omics of human plasma reveals molecular features of dysregulated

inflammation and accelerated aging in schizophrenia. *Mol Psychiatry.* 2022;27(2):1217–1225. doi:10.1038/s41380-021-01339-z

33. Mihaljević-Peleš A, Bajs Janović M, Šagud M, Živković M, Janović S, Jevtović S. Cognitive deficit in schizophrenia: an overview. *Psychiatr Danub.* 2019;31(Suppl 2):139–142.
34. Olfson M, Gerhard T, Huang C, Crystal S, Stroup TS. Premature mortality among adults with schizophrenia in the United States. *JAMA Psychiatry*. 2015;72(12):1172–1181. doi:10.1001/jamapsychiatry.2015.1737
35. Laursen TM. Causes of premature mortality in schizophrenia: a review of literature published in 2018. *Curr Opin Psychiatry.* 2019;32(5):388–393. doi:10.1097/YCO.0000000000000530
36. Hjorthøj C, Stürup AE, McGrath JJ, Nordentoft M. Years of potential life lost and life expectancy in schizophrenia: a systematic review and meta-analysis. *The Lancet Psychiatry*. 2017;4(4):295–301. doi:10.1016/S2215-0366(17)30078-0
37. Pillinger T, Beck K, Gobjila C, Donocik JG, Jauhar S, Howes OD. Impaired glucose homeostasis in first-episode schizophrenia: a systematic review and meta-analysis. *JAMA Psychiatry*. 2017;74(3):261–269. doi:10.1001/jamapsychiatry.2016.3803
38. Heald A, Pendlebury J, Anderson S, et al. Lifestyle factors and the metabolic syndrome in Schizophrenia: a cross-sectional study. *Ann Gen Psychiatry*. 2017;16(1):12. doi:10.1186/s12991-017-0134-6
39. Mitchell AJ, Vancampfort D, Sweers K, Van Winkel R, Yu W, De Hert M. Prevalence of metabolic syndrome and metabolic abnormalities in schizophrenia and related disorders—a systematic review and meta-analysis. *Schizophr Bull.* 2013;39(2):306–318. doi:10.1093/schbul/sbr148
40. Wu YF, Sytwu HK, Lung FW. Polymorphisms in the human aquaporin 4 gene are associated with schizophrenia in the Southern Chinese ham population: a case–control study. *Front Psychiatry.* 2020;11:596. doi:10.3389/fpsyt.2020.00596
41. Saarinen A, Lieslehto J, Kiviniemi V, et al. Symptomatic psychosis risk and physiological fluctuation in functional MRI data. *Schizophr Res.* 2020;216:339–346. doi:10.1016/j.schres.2019.11.029
42. Wilson RS, Segawa E, Boyle PA, Anagnos SE, Hizel LP, Bennett DA. The natural history of cognitive decline in Alzheimer's disease. *Psychol Aging.* 2012;27(4):1008–1017. doi:10.1037/a0029857
43. Zahodne LB, Manly JJ, MacKay-Brandt A, Stern Y. Cognitive Declines Precede and Predict Functional Declines in Aging and Alzheimer's Disease. Hashimoto K, ed. *PLoS One.* 2013;8(9):e73645. doi:10.1371/journal.pone.0073645
44. Liang CS, Li DJ, Yang FC, et al. Mortality rates in Alzheimer's disease and non-Alzheimer's dementias: a systematic review and meta-analysis. *Lancet Healthy Longevity*. 2021;2(8):e479–e488. doi:10.1016/S2666-7568(21)00140-9
45. Cai H, Cong W, Ji S, Rothman S, Maudsley S, Martin B. Metabolic dysfunction in Alzheimers disease and related neurodegenerative disorders. *CAR*. 2012;9(1):5–17. doi:10.2174/156720512799015064
46. Muddapu VR, Dharshini SAP, Chakravarthy VS, Gromiha MM. Neurodegenerative diseases – Is metabolic deficiency the root cause? *Front Neurosci.* 2020;14:213. doi:10.3389/fnins.2020.00213
47. Leparulo A, Bisio M, Redolfi N, Pozzan T, Vassanelli S, Fasolato C. Accelerated aging characterizes the early stage of Alzheimer's disease. *Cells*. 2022;11(2):238. doi:10.3390/cells11020238
48. Burfeind KG, Murchison CF, Westaway SK, et al. The effects of noncoding aquaporin-4 single-nucleotide polymorphisms on cognition and functional progression of Alzheimer's disease. *A&D Transl Res & Clin Interv*. 2017;3(3):348–359. doi:10.1016/j.trci.2017.05.001
49. Chandra A, Farrell C, Wilson H, Dervenoulas G, De Natale ER, Politis M; Alzheimer's Disease Neuroimaging Initiative. Aquaporin-4 polymorphisms predict amyloid burden and clinical outcome in the Alzheimer's disease spectrum. *Neurobiol Aging.* 2021;97:1–9. doi:10.1016/j.neurobiolaging.2020.06.007
50. Chung CP, Lee HY, Lin PC, Wang PN. Cerebral artery pulsatility is associated with cognitive impairment and predicts dementia in individuals with subjective memory decline or mild cognitive impairment. *JAD*. 2017;60(2):625–632. doi:10.3233/JAD-170349
51. Li Y, Zhou Y, Zhong W, et al. Choroid plexus enlargement exacerbates white matter hyperintensity growth through glymphatic impairment. *Ann Neurol.* 2023;94(1):182–195. doi:10.1002/ana.26648
52. Lizano P, Lutz O, Ling G, et al. Association of choroid plexus enlargement with cognitive, inflammatory, and structural phenotypes across the psychosis spectrum. *Am J Psychiatry.* 2019;176(7):564–572. doi:10.1176/appi.ajp.2019.18070825
53. Yakimov V, Moussiopoulou J, Roell L, et al. Investigation of choroid plexus variability in schizophrenia-spectrum disorders – insights from a multimodal stud. Published online 2023. doi:10.1101/2023.12.18.23300130
54. Eide PK, Ringstad G. MRI with intrathecal MRI gadolinium contrast medium administration: a possible method to assess glymphatic function in human brain. *Acta Radiol Open*. 2015;4(11):2058460115609635. doi:10.1177/2058460115609635
55. Naganawa S, Nakane T, Kawai H, Taoka T. Gd-based contrast enhancement of the perivascular spaces in the Basal Ganglia. *Magn Reson Med Sci.* 2017;16(1):61–65. doi:10.2463/mrms.mp.2016-0039
56. Besteher B, Chung HY, Mayer TE, Witte OW, Kirchhof K, Schwab M. Acute encephalopathy and cardiac arrest induced by intrathecal gadolinium administration. *Clin Neuroradiol*. 2020;30(3):629–631. doi:10.1007/s00062-019-00845-6
57. Provenzano DA, Pellis Z, DeRiggi L. Fatal gadolinium-induced encephalopathy following accidental intrathecal administration: a case report and a comprehensive evidence-based review. *Reg Anesth Pain Med.* 2019;44:721–729. doi:10.1136/rapm-2019-100422
58. Li L, Gao FQ, Zhang B, Luo BN, Yang ZY, Zhao J. Overdosage of intrathecal gadolinium and neurological response. *Clin Radiol.* 2008;63(9):1063–1068. doi:10.1016/j.crad.2008.02.004
59. Patel M, Atyani A, Salameh JP, McInnes M, Chakraborty S. Safety of intrathecal administration of gadolinium-based contrast agents: a systematic review and meta-analysis. *Radiology.* 2020;297(1):75–83. doi:10.1148/radiol.2020191373
60. Cudalbu C, Behar KL, Bhattacharyya PK, et al. Contribution of macromolecules to brain 1 H MR spectra: Experts' consensus recommendations. *NMR Biomed.* 2021;34(5):e4393. doi:10.1002/nbm.4393
61. Howe FA, Barton SJ, Cudlip SA, et al. Metabolic profiles of human brain tumors using quantitative in vivo ^{1}H magnetic resonance spectroscopy. *Magnetic Resonance Med.* 2003;49(2):223–232. doi:10.1002/mrm.10367
62. Seeger U, Klose U, Mader I, Grodd W, Nägele T. Parameterized evaluation of macromolecules and lipids

in proton MR spectroscopy of brain diseases. *Magnetic Resonance Med*. 2003;49(1):19–28. doi:10.1002/mrm.10332

63. Mader I, Seeger U, Weissert R, et al. Proton MR spectroscopy with metabolite-nulling reveals elevated macromolecules in acute multiple sclerosis. *Brain.* 2001;124(5):953–961. doi:10.1093/brain/124.5.953
64. Stadtman ER. Protein oxidation and aging. *Free Radic Res.* 2006;40(12):1250–1258. doi:10.1080/10715760600918142
65. Nguyen TT, Eyler LT, Jeste DV. Systemic biomarkers of accelerated aging in schizophrenia: a critical review and future directions. *Schizophr Bull.* 2018;44(2):398–408. doi:10.1093/schbul/sbx069
66. Hsiao WC, Chang HI, Hsu SW, et al. Association of cognition and brain reserve in aging and glymphatic function using diffusion tensor image-along the perivascular space (DTI-ALPS). *Neuroscience.* 2023;524:11–20. doi:10.1016/j.neuroscience.2023.04.004
67. Bell CC. DSM-IV: diagnostic and statistical manual of mental disorders. *JAMA.* 1994;272(10):828. doi:10.1001/jama.1994.03520100096046
68. Sheehan DV, Lecrubier Y, Sheehan KH, et al. The Mini-International Neuropsychiatric Interview (M.I.N.I.): the development and validation of a structured diagnostic psychiatric interview for DSM-IV and ICD-10. *J Clin Psychiatry.* 1998;59:22–33;quiz 34.
69. Iwata Y, Nakajima S, Plitman E, et al. Glutamatergic neurometabolite levels in patients with ultra-treatment-resistant schizophrenia: a cross-sectional 3T proton magnetic resonance spectroscopy study. *Biol Psychiatry.* 2019;85(7):596–605. doi:10.1016/j.biopsych.2018.09.009
70. Iwata Y, Nakajima S, Plitman E, et al. Glutathione levels and glutathione-glutamate correlation in patients with treatment-resistant schizophrenia. *Schizophr. Bull. Open.* 2021;2(1):sgab006. doi:10.1093/schizbullopen/sgab006
71. van Engelen MPE, Verfaillie SCJ, Dols A, et al. Altered brain metabolism in frontotemporal dementia and psychiatric disorders: involvement of the anterior cingulate cortex. *EJNMMI Res*. 2023;13(1):71. doi:10.1186/s13550-023-01020-2
72. Yuan Q, Liang X, Xue C, et al. Altered anterior cingulate cortex subregional connectivity associated with cognitions for distinguishing the spectrum of pre-clinical Alzheimer's disease. *Front Aging Neurosci.* 2022;14:1035746. doi:10.3389/fnagi.2022.1035746
73. Xiong Y, Ye C, Chen Y, et al. Altered Functional connectivity of basal ganglia in mild cognitive impairment and Alzheimer's disease. *Brain Sci*. 2022;12(11):1555. doi:10.3390/brainsci12111555
74. Zheng W, Liu X, Song H, Li K, Wang Z. Altered functional connectivity of cognitive-related cerebellar Subregions in Alzheimer's disease. *Front Aging Neurosci.* 2017;9:143. doi:10.3389/fnagi.2017.00143
75. Kumar S, Zomorrodi R, Ghazala Z, et al. Extent of dorsolateral prefrontal cortex plasticity and its association with working memory in patients with Alzheimer disease. *JAMA Psychiatry*. 2017;74(12):1266–1274. doi:10.1001/jamapsychiatry.2017.3292
76. Chang HI, Huang CW, Hsu SW, et al. Gray matter reserve determines glymphatic system function in young-onset Alzheimer's disease: evidenced by DTI-ALPS and compared with age-matched controls. *Psychiatry Clin Neurosci.* 2023;77(7):401–409. doi:10.1111/pcn.13557
77. Feng N, Palaniyappan L, Robbins TW, et al. Working memory processing deficit associated with a nonlinear response pattern of the anterior cingulate cortex in first-episode and drug-naïve schizophrenia. *Neuropsychopharmacology.* 2023;48(3):552–559. doi:10.1038/s41386-022-01499-8
78. Li A, Zalesky A, Yue W, et al. A neuroimaging biomarker for striatal dysfunction in schizophrenia. *Nat Med.* 2020;26(4):558–565. doi:10.1038/s41591-020-0793-8
79. O'Neill A, Mechelli A, Bhattacharyya S. Dysconnectivity of large-scale functional networks in early psychosis: a meta-analysis. *Schizophr Bull.* 2019;45(3):579–590. doi:10.1093/schbul/sby094
80. Sekiguchi H, Pavey G, Dean B. Altered levels of dopamine transporter in the frontal pole and dorsal striatum in schizophrenia. *npj Schizophr.* 2019;5:20. doi:10.1038/s41537-019-0087-7
81. Brugger SP, Howes OD. Heterogeneity and homogeneity of regional brain structure in schizophrenia: a meta-analysis. *JAMA Psychiat*. 2017;74(11):1104–1111. doi:10.1001/jamapsychiatry.2017.2663
82. Mucci A, Dima D, Soricelli A, et al. Is avolition in schizophrenia associated with a deficit of dorsal caudate activity? A functional magnetic resonance imaging study during reward anticipation and feedback. *Psychol Med.* 2015;45(8):1765–1778. doi:10.1017/S0033291714002943
83. Barch DM, Ceaser A. Cognition in schizophrenia: core psychological and neural mechanisms. *Trends Cogn Sci.* 2012;16(1):27–34. doi:10.1016/j.tics.2011.11.015
84. Fornito A, Yücel M, Dean B, Wood SJ, Pantelis C. Anatomical abnormalities of the anterior cingulate cortex in schizophrenia: bridging the gap between neuroimaging and neuropathology. *Schizophr Bull.* 2009;35(5):973–993. doi:10.1093/schbul/sbn025
85. Yoon JH, Minzenberg MJ, Ursu S, et al. Association of dorsolateral prefrontal cortex dysfunction with disrupted coordinated brain activity in schizophrenia: relationship with impaired cognition, behavioral disorganization, and global function. *Am J Psychiat.* 2008;165(8):1006–1014. doi:10.1176/appi.ajp.2008.07060945
86. Patenaude B, Smith SM, Kennedy DN, Jenkinson M. A Bayesian model of shape and appearance for subcortical brain segmentation. *Neuroimage.* 2011;56(3):907–922. doi:10.1016/j.neuroimage.2011.02.046
87. Woolrich MW, Jbabdi S, Patenaude B, et al. Bayesian analysis of neuroimaging data in FSL. *Neuroimage.* 2009;45(1):S173–S186. doi:10.1016/j.neuroimage.2008.10.055
88. Provencher SW. Automatic quantitation of localized in vivo ^{1}H spectra with LCModel. *NMR Biomed.* 2001;14(4):260–264. doi:10.1002/nbm.698
89. Smith SM. Fast robust automated brain extraction. *Hum Brain Mapp.* 2002;17(3):143–155. doi:10.1002/hbm.10062
90. Andersson JLR, Sotiropoulos SN. An integrated approach to correction for off-resonance effects and subject movement in diffusion MR imaging. *Neuroimage.* 2016;125:1063–1078. doi:10.1016/j.neuroimage.2015.10.019
91. Andersson JLR, Graham MS, Zsoldos E, Sotiropoulos SN. Incorporating outlier detection and replacement into a non-parametric framework for movement and distortion correction of diffusion MR images. *Neuroimage.* 2016;141:556–572. doi:10.1016/j.neuroimage.2016.06.058
92. Tatekawa H, Matsushita S, Ueda D, et al. Improved reproducibility of diffusion tensor image analysis along the perivascular space (DTI-ALPS) index: an analysis of reorientation technique of the OASIS-3 dataset. *Jpn J Radiol*. 2023;41(4):393–400. doi:10.1007/s11604-022-01370-2

93. Jenkinson M, Smith S. A global optimisation method for robust affine registration of brain images. *Med Image Anal.* 2001;5(2):143–156. doi:10.1016/S1361-8415(01)00036-6
94. Jenkinson M, Bannister P, Brady M, Smith S. Improved optimization for the robust and accurate linear registration and motion correction of brain images. *Neuroimage.* 2002;17(2):825–841. doi:10.1006/nimg.2002.1132
95. Taoka T, Ito R, Nakamichi R, et al. Reproducibility of diffusion tensor image analysis along the perivascular space (DTI-ALPS) for evaluating interstitial fluid diffusivity and glymphatic function: CHanges in Alps index on Multiple conditiON acquIsition eXperiment (CHAMONIX) study. *Jpn J Radiol*. 2022;40(2):147–158. doi:10.1007/s11604-021-01187-5
96. Okudera T, Huang YP, Fukusumi A, Nakamura Y, Hatazawa J, Uemura K. Micro-angiographical studies of the medullary venous system of the cerebral hemisphere. *Neuropathology*. 1999;19(1):93–111. doi:10.1046/j.1440-1789.1999.00215.x
97. Tukey JW, John W. Exploratory data analysis. Accessed February 15, 2024. https://cir.nii.ac.jp/crid/1130282268675601280
98. Faul F, Erdfelder E, Buchner A, Lang AG. Statistical power analyses using G*Power 3.1: Tests for correlation and regression analyses. *Behav Res Methods.* 2009;41(4):1149–1160. doi:10.3758/BRM.41.4.1149
99. Kay SR, Fiszbein A, Opler LA. The Positive and Negative Syndrome Scale (PANSS) for Schizophrenia. *Schizophr Bull.* 1987;13(2):261–276. doi:10.1093/schbul/13.2.261
100. Saleem S, Shaukat F, Gul A, Arooj M, Malik A. Potential role of amino acids in pathogenesis of schizophrenia. *Int J Health Sci (Qassim)*. 2017;11(3):63–68.
101. Fernstrom JD. Dietary precursors and brain neurotransmitter formation. *Annu Rev Med.* 1981;32:413–425. doi:10.1146/annurev.me.32.020181.002213
102. Luvsannyam E, Jain MS, Pormento MKL, et al. Neurobiology of schizophrenia: a comprehensive review. *Cureus*. 2022;14(4):e23959. doi:10.7759/cureus.23959
103. Lahti AC, Koffel B, LaPorte D, Tamminga CA. Subanesthetic doses of ketamine stimulate psychosis in schizophrenia. *Neuropsychopharmacology.* 1995;13(1):9–19. doi:10.1016/0893-133X(94)00131-I
104. Krystal JH, Karper LP, Seibyl JP, et al. Subanesthetic effects of the noncompetitive NMDA antagonist, ketamine, in humans. Psychotomimetic, perceptual, cognitive, and neuroendocrine responses. *Arch Gen Psychiatry.* 1994;51(3):199–214. doi:10.1001/archpsyc.1994.03950030035004
105. Marsman A, van den Heuvel MP, Klomp DWJ, Kahn RS, Luijten PR, Hulshoff Pol HE. Glutamate in schizophrenia: a focused review and meta-analysis of ^{1}H-MRS studies. *Schizophr Bull.* 2013;39(1):120–129. doi:10.1093/schbul/sbr069
106. Merritt K, McCutcheon RA, Aleman A, et al; 1H-MRS in Schizophrenia Investigators. Variability and magnitude of brain glutamate levels in schizophrenia: a meta and mega-analysis. *Mol Psychiatry.* 2023;28(5):2039–2048. doi:10.1038/s41380-023-01991-7
107. Charidimou A, Hong YT, Jäger HR, et al. White matter perivascular spaces on magnetic resonance imaging: marker of cerebrovascular amyloid burden? *Stroke.* 2015;46(6):1707–1709. doi:10.1161/STROKEAHA.115.009090
108. Charidimou A, Meegahage R, Fox Z, et al. Enlarged perivascular spaces as a marker of underlying arteriopathy in intracerebral haemorrhage: a multicentre MRI cohort study. *J Neurol Neurosurg Psychiatry.* 2013;84(6):624–629. doi:10.1136/jnnp-2012-304434
109. Kamagata K, Andica C, Takabayashi K, et al; Alzheimer's Disease Neuroimaging Initiative. Association of MRI Indices of Glymphatic System With Amyloid Deposition and Cognition in Mild Cognitive Impairment and Alzheimer Disease. *Neurology.* 2022;99(24):e2648–e2660. doi:10.1212/WNL.0000000000201300
110. Gouveia-Freitas K, Bastos-Leite AJ. Perivascular spaces and brain waste clearance systems: relevance for neurodegenerative and cerebrovascular pathology. *Neuroradiology.* 2021;63(10):1581–1597. doi:10.1007/s00234-021-02718-7
111. De Oliveira Figueiredo EC, Calì C, Petrelli F, Bezzi P. Emerging evidence for astrocyte dysfunction in schizophrenia. *Glia.* 2022;70(9):1585–1604. doi:10.1002/glia.24221
112. Mäki-Marttunen V, Andreassen OA, Espeseth T. The role of norepinephrine in the pathophysiology of schizophrenia. *Neurosci Biobehav Rev.* 2020;118:298–314. doi:10.1016/j.neubiorev.2020.07.038
113. Berridge CW, Waterhouse BD. The locus coeruleus-noradrenergic system: modulation of behavioral state and state-dependent cognitive processes. *Brain Res Brain Res Rev.* 2003;42(1):33–84. doi:10.1016/s0165-0173(03)00143-7
114. Jones BE. Arousal and sleep circuits. *Neuropsychopharmacol*. 2020;45(1):6–20. doi:10.1038/s41386-019-0444-2
115. Oishi Y, Lazarus M. The control of sleep and wakefulness by mesolimbic dopamine systems. *Neurosci Res.* 2017;118:66–73. doi:10.1016/j.neures.2017.04.008
116. Kesby JP, Eyles DW, McGrath JJ, Scott JG. Dopamine, psychosis and schizophrenia: the widening gap between basic and clinical neuroscience. *Transl Psychiatry.* 2018;8(1):30. doi:10.1038/s41398-017-0071-9
117. Hietala J, Syvälahti E, Vuorio K, et al. Presynaptic dopamine function in striatum of neuroleptic-naive schizophrenic patients. *Lancet.* 1995;346(8983):1130–1131. doi:10.1016/s0140-6736(95)91801-9
118. Seeman P, Lee T. Antipsychotic drugs: direct correlation between clinical potency and presynaptic action on dopamine neurons. *Science.* 1975;188(4194):1217–1219. doi:10.1126/science.1145194
119. Monti JM, BaHammam AS, Pandi-Perumal SR, et al. Sleep and circadian rhythm dysregulation in schizophrenia. *Prog Neuropsychopharmacol Biol Psychiatry.* 2013;43:209–216. doi:10.1016/j.pnpbp.2012.12.021
120. Saito Y, Hayakawa Y, Kamagata K, et al. Glymphatic system impairment in sleep disruption: diffusion tensor image analysis along the perivascular space (DTI-ALPS). *Jpn J Radiol*. 2023;41:1335–1343. doi:10.1007/s11604-023-01463-6